MolGround: A Benchmark for Molecular Grounding

Jiaxin Wu[1], Ting Zhang[1], Rubing Chen[1], Wengyu Zhang[1],
Chen Jason Zhang[1], Xiaoyong Wei[2,1,*], Li Qing[1],
[1]The Hong Kong Polytechnic University, [2]Sichuan University,

arXiv:2503.23668v3 [cs.AI] 12 Apr 2025

Abstract

Current molecular understanding approaches predominantly focus on the descriptive aspect of human perception, providing broad, topic-level insights. However, the referential aspect—linking molecular concepts to specific structural components—remains largely unexplored. To address this gap, we propose a molecular grounding benchmark designed to evaluate a model's referential abilities. We align molecular grounding with established conventions in NLP, cheminformatics, and molecular science, showcasing the potential of NLP techniques to advance molecular understanding within the AI for Science movement. Furthermore, we constructed the largest molecular understanding benchmark to date, comprising 117k QA pairs, and developed a multi-agent grounding prototype as proof of concept. This system outperforms existing models, including GPT-4o, and its grounding outputs have been integrated to enhance traditional tasks such as molecular captioning and ATC (Anatomical, Therapeutic, Chemical) classification.

1 Introduction

Deep learning models have transformed traditional molecular understanding tasks, including property prediction (Wu et al., 2017; Walters and Barzilay, 2021; Zhang et al., 2024b), molecular generation (Xu et al., 2019; Hua et al., 2024; Song et al., 2024), and reaction prediction (Fooshee et al., 2018; Ding et al., 2024; Tavakoli et al., 2024). Recently, tasks like molecular captioning (Edwards et al., 2021) and molecule-language translation (Edwards et al., 2024) have gained significant attention due to advancements in large language models (Li et al., 2024; Pei et al., 2024). These models represent molecular structures as sequences of tokens, enabling the generation of natural language descriptions by leveraging sophisticated sequence-to-sequence learning techniques.

While having yielded promising results, these approaches primarily mimic the **descriptive** aspect of human perception (Cocchiarella, 1974; Geach, 1950; Kamp and Reyle, 1993), focusing on broad, topic-level understanding. The **referential** aspect of perception, which associates concepts with specific molecular components (e.g., atoms, functional groups, rings), has been overlooked. For example, consider the SMILES *CC(=O)O* (*acetic acid*). In molecular captioning, a typical output might be: "This is acetic acid, commonly known as the main component of vinegar. It is used industrially in production and exhibits toxic effects at high concentrations." While this description is highly informative, it is descriptive in nature. From a referential perspective, it is more critical to identify which specific part of the molecule contributes to its toxicity. In this case, the *carbonyl group (C=O)* is responsible for the molecule's corrosive effects, as it facilitates the release of protons *(H+)*, which can damage biological tissues. This referential understanding not only enhances interpretability but also generalizes to other similar compounds, such as *formic acid*, *oxalic acid*, and *trichloroacetic acid*.

While the complementary nature of descriptive and referential perceptions has long been modeled in cognitive science, such as in Fregean Semantics (Cocchiarella, 1974), Russell's Theory of Descriptions (Geach, 1950), and Discourse Representation Theory (DRT) by Hans Kamp and Uwe Reyle (Kamp and Reyle, 1993), it has also been successfully implemented recently in vision-language research (Arai and Tsugawa, 2024; Liu et al., 2023). The integration of visual grounding (Xiao et al., 2024; Deng et al., 2021), which mimics referential perception by linking textual concepts to specific image regions, has significantly advanced the performance, interpretability, and generalization of vision-language models. These models, which traditionally relied solely on image-caption pairs for training, have greatly benefited from this approach.

*Corresponding Author

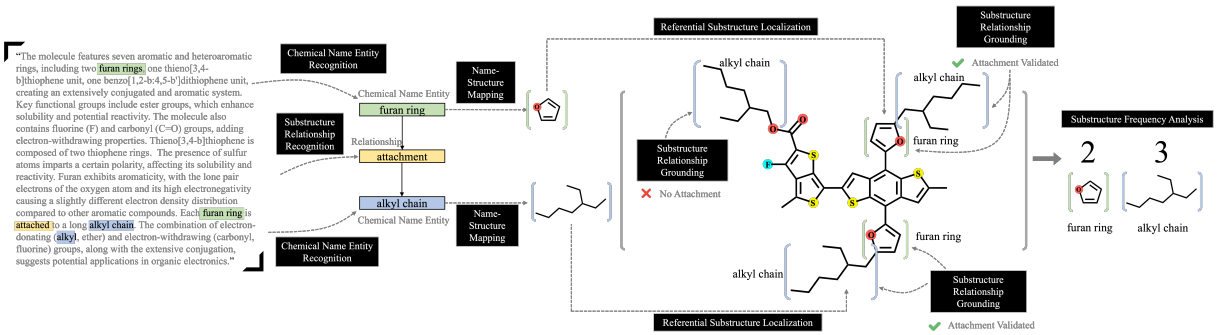

Figure 1: A referential framework for fine-grained molecular grounding, comprising five tasks: Chemical Name Entity Recognition, Name-Structure Mapping, Referential Substructure Localization, Substructure Relationship Grounding, and Substructure Frequency Analysis, demonstrated through a running example.

Believing that molecular understanding research is at a similar turning point, we propose a grounding benchmark to assess a model's ability to explicitly associate molecular concepts with specific structural components. This benchmark emphasizes fine-grained understanding and interpretability, enabling models to identify, explain, and reason about the roles of particular molecular features. Unlike visual grounding, where a model is primarily tasked with identifying the locations of concepts, molecular grounding requires the identification of specified components at multiple cognitive levels, including concept instances, structural locations, and compositional facts. From a pragmatics perspective, molecular grounding differs from existing molecular understanding tasks that focus on the topic. Instead, it emphasizes providing answers to fine-grained queries such as "What?", "Where?", and "Which ones?". Figure 1 illustrates the proposed molecular grounding tasks including Chemical Name Entity Recognition (CNER), Name-Structure Mapping (NSM), Referential Substructure Localization (RSL), Substructure Relationship Grounding (SRG), and Substructure Frequency Analysis (SFA). This paper serves as a pilot study aimed at formulating molecular grounding by aligning it with established conventions in NLP, cheminformatics, and molecular science. Our findings demonstrate that NLP techniques can play a critical role in advancing molecular understanding within the broader AI for Science movement. In addition to creating the largest molecular understanding benchmark to date, we developed a multi-agent grounding prototype as a proof of concept. This system outperforms existing models, such as GPT-4o (OpenAI et al., 2024), and its grounding results have been successfully integrated to enhance conventional tasks like molecular captioning and ATC (anatomical, therapeutic, chemical) classification.

2 Related Work

Molecular understanding has been a long-standing field of research, predating the recent surge of interest in AI for Science. The tasks in this field can be broadly grouped into three categories based on their popularity: 1) Property prediction (Wu et al., 2017; Walters and Barzilay, 2021; Zhang et al., 2024a) and representation learning (Fang et al., 2022b; Zhang et al., 2024b), which are the most extensively studied and widely popular. 2) Structure prediction (John Jumper et al., 2021; Song et al., 2024), captioning (Li et al., 2024; Edwards et al., 2021), and generation (Xu et al., 2019; Hua et al., 2024), which have recently gained significant attention. 3) Emerging studies on tasks such as reaction prediction and optimization (Fooshee et al., 2018), interaction prediction (Tavakoli et al., 2024), simulations and dynamics (Vander Meersche et al., 2024), toxicity and safety assessment (Sahu and Poler, 2024), and visualization and explainability (Janissen et al., 2024). The popularity of the first two groups largely stems from the ease of directly applying sophisticated machine learning models to these tasks. Early approaches relied on methods like Bayesian classifiers (Langley et al., 1992), logistic regression (Hosmer Jr et al., 2013), and SVMs (Hearst et al., 1998), while more recent efforts have widely adopted CNNs (O'Shea, 2015), GNNs (Wu et al., 2020), and Transformer-based models (Vaswani, 2017). Most of these models follow a pipeline of encoding molecules into embeddings and predicting outputs such as labels or textual descriptions, reflecting the way these models were initially designed. However,

these implementations tend to be **descriptive**, as they focus on high-level concepts by treating a molecule as a whole, rather than addressing its internal components. The third group, on the other hand, signals a shift toward more fine-grained modeling and improved interpretability. This shift is driven by two factors: 1) The needs of identifying subcomponents in molecular science, such as reaction tracing (Smith and March, 2007; Fang et al., 2022a; Umit V. Ucak and Lee, 2021) and understanding molecule-target interactions (Lipinski et al., 1997; Segler et al., 2018). 2) Advancements in machine learning for interpretability and generalization (Gao and Guan, 2023). Ultimately, these developments highlight the growing demand for models with **referential** perception, enabling them to go beyond high-level descriptions and address specific components within a molecule.

The complementary relationship between descriptive and referential perceptions has been extensively explored in cognitive science, as seen in Fregean Semantics (senses and references) (Cocchiarella, 1974), Russell's Theory of Descriptions (definite descriptions and proper names) (Geach, 1950), and Discourse Representation Theory (descriptions and referents) (Kamp and Reyle, 1993). However, referential perception has not been explicitly modeled or systematically evaluated in molecular understanding. From this perspective, Table 1 summarizes advanced models such as BioT5 (Pei et al., 2024), ChemLLM (Zhang et al., 2024a), and Mol-Instructions (Fang et al., 2024), alongside commonly adopted benchmarks like ChemBench4K (Zhang et al., 2024a), and MoleculeQA (Lu et al., 2024). It is clear that this is an area requiring more focused and explicit attention. While recent advancements in models have made strides toward incorporating referential perception, with promising results observed in integrating referential perception-oriented visual grounding (e.g., RefFormer (Wang et al., 2024), ClawMachine (Ma et al., 2024), DOrA (Wu et al., 2024)), significant challenges remain. This results from the heavy reliance on costly human expertise for benchmark construction and the lack of a systematic formulation of the problem. As highlighted in Table 1 , our proposed MolGround represents an initial effort to address these challenges. It scales up to 1.91 times larger than existing benchmarks and introduces fine-grained definitions to better align with the requirements of referential perception.

Benchmarks	Tasks	#QA	#Des.(%)	#Ref.(%)
CB4	Caption2mol	800	97.75	2.25
	Mol2Caption	299	100.00	0.00
	Name Conversion	799	99.87	0.13
	Product Prediction	300	96.99	3.01
	Yield Prediction	300	100.00	0.00
	Temperature Prediction	202	98.98	1.02
	Solvent Prediction	300	87.66	12.34
	Retrosynthesis	300	96.00	4.00
	Property Prediction	709	59.23	40.77
	Total	4,009	90.88	9.12
MQA	Preperty	6,267	100.00	0.00
	Usage	3,074	100.00	0.00
	Source	13,630	100.00	0.00
	Structure	38,603	83.62	16.38
	Total	61,574	91.19	8.81
MolGround (ours)	Name Entity (CNER)	15,033	0.00	100.00
	Name2Struct (BNSM)	1,397	100.00	0.00
	Localization (RSL)	48,107	0.00	100.00
	Grounding (SRG)	13,994	0.00	100.00
	Analysis (SFA)	38,780	0.00	100.00
	Total	**117,311**	1.19	**98.81**

Table 1: Question-answer pair distribution across descriptive (Des.) and referential (Ref.) perceptions, covering benchmarks ChemBench4K (CB4), MoleculeQA (MQA), and MolGround (Ours).

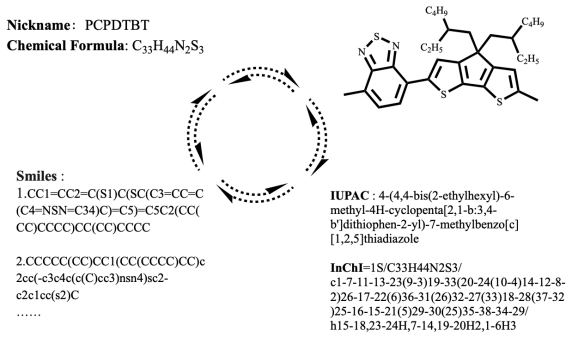

Figure 2: Diversity in naming conventions and multimodal gaps between the textual and structural forms.

3 Molecular Grounding Tasks

We define 5 groups of grounding tasks by aligning to the common conventions in NLP, cheminformatics, and molecular science. The alignment and challenges of each task are summarized in Table 2.

Chemical Named Entity Recognition (CNER): *Recognize and extract chemical entity names (e.g., molecule names, substructure names, or functional groups) as a set $\mathcal{N}$ from a given caption $\mathcal{X}$ as*

$$f_N : \mathcal{X} \mapsto \mathcal{N} \qquad \mathcal{X} = \{x_i\}, \mathcal{N} = \{n_j\} \tag{1}$$

where x_i is the ith token in the sequence $\mathcal{X}$, and n_j is a quadruple (c_j, b_j, l_j, r_j) consisting of the jth extracted name entity c_j and its role $r_j \in \mathcal{R}$, beginning position $0 \leq b_j \leq \|X\|$, and length l_j. Note $\mathcal{R}$ is a set of predefined roles (e.g., donor, acceptor) which are contextual and application-specific.

Cognitive levels	Tasks	Challenges	Required Abilities
Remember	CNER	Diverse Entity Forms	Chemical Knowledge Recall; Syntax Understanding
Understand	BNSM	Multimodal Transformation;	Semantic Understanding; Syntax Understanding
Apply	SFA-Atom	Multi-instances; Coreference Resolution	Substructure Matching; Pattern Recognition
Analyze	SFA-Heteroatoms Type	Similarity Differentiation	Semantic Understanding; Categorization
	SFA-Monocyclic Ring Type	Structural Similarity;	Pattern Recognition; Categorization
	SFA-Non-exist Ring	Absence Detection	Negative Pattern Recognition;
	SRG	Multidimensional Relations	Structural Understanding; Relationship Inference
	Singular RSL	Multi-instances	Spatial Reasoning; Pattern Recognition
Evaluate	SFA-Ring	Multiple Representation forms	Structural Comparison; Quantitative Analysis
	SFA-Substructure	Structural Variability;	Pattern Recognition; Logical Deduction
	Multiple RSL	Multiple Structures; Diverse Relation Types	Contextual Reasoning

Table 2: Grounding tasks with Bloom's Cognitive Levels, corresponding challenges, and required abilities.

This task reflects referential perception by linking textual mentions of chemical entities to their semantic roles and serves as a foundation for molecular grounding by identifying key entities for downstream tasks. While similar to Named Entity Recognition (NER) in NLP, CNER extends the task by additionally identifying the roles of extracted entities. Furthermore, unlike NER, where entities are typically proper nouns or noun phrases, chemical entities are significantly more diverse and technically complex. For instance, the *drug acetaminophen* exemplifies this complexity: it has multiple IUPAC names, such as *N-(4-hydroxyphenyl)acetamide*, *4'-hydroxyacetanilide*, and *p-hydroxyacetanilide*; a molecular formula, *C8H9NO2*; an InChI representation, *InChI=1S/C8H9NO2/c1-6(10)9-7-2-4-8(11)5-3-7/h2-5,11H,1H3,(H,9,10)*; as well as various SMILES representations and trade names like *Tylenol*, *Panadol*, and *Calpol*. As illustrated in Figure 2, a CNER model must accommodate these diverse forms, demanding the ability to recall chemical domain knowledge and a deep understanding of chemical syntax and representation conventions.

Bidirectional Name-Structure Mapping (BNSM): *Translate chemical names $\mathcal{N}$ into corresponding structural representations (e.g., SMILES, InChI, molecular graphs) $\mathcal{S}$ or convert given structural representations back into their corresponding names as*

$$\begin{aligned} f_{n2s} &: \mathcal{N} \mapsto \mathcal{S} \\ f_{s2n} &: \mathcal{S} \mapsto \mathcal{N} \\ &\mathcal{N} = \{n_i\},\ \mathcal{S} = \{s_j\} \end{aligned} \tag{2}$$

where structural representation $\mathcal{S}$ is sequences of textual codes in SMILES, InChI, or molecular graphs wrapping atoms (nodes) and bonds (edges).

This task bridges textual and structural representations, embodying referential perception by grounding a molecule's name to its physical structure and vice versa. It aligns with translation tasks in NLP and structure-based prediction tasks in cheminformatics. As illustrated in Figure 2, unlike the sequence-to-sequence framework used in NLP translation, this task introduces an additional multimodal challenge. This complexity arises from the hierarchical and graph-based nature of molecular structures, which are governed by spatial and chemical constraints. Furthermore, this task has extremely low error tolerance, as even a minor mistake in structure representation can lead to a fundamentally different molecule (e.g., *C1=CC=CC=C1* vs. *C1=NC=CC=C1*).

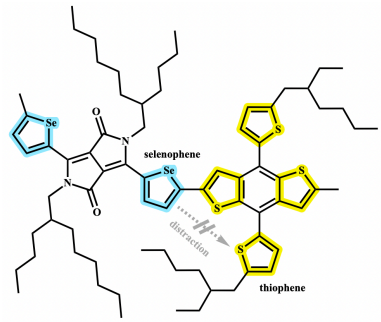

Figure 3: Multiple instances of *thiophene* rings, varying by rotations, present a challenge in identifying a generalizable feature for localization. Additionally, *selenophene* rings, differing by only one atom from *thiophene*, may further complicate localization.

Referential Substructure Localization (RSL): *Identify the specific occurrences of substructures (e.g., functional groups, rings, or atoms) within a molecule's structural representation $\mathcal{G}$, based on their names or descriptions $\mathcal{N}$ as*

$$\begin{aligned} f_L &: (\mathcal{N}, \mathcal{G}) \mapsto \mathcal{L} \\ &\mathcal{N} = \{n_i\},\ \mathcal{G} = (\mathcal{V}, \mathcal{E}),\ \mathcal{G}_i \subseteq \mathcal{G}, \\ &\mathcal{L} = \{\mathcal{L}_i\} \in \{\mathcal{G}_i\} \times \mathcal{G} \end{aligned} \tag{3}$$

where $\mathcal{V}$ is the set of atoms (nodes) and $\mathcal{E}$ is the set

of bonds (edges), $\mathcal{G}_i = (\mathcal{V}_i, \mathcal{E}_i)$ is the substructure graph for n_i, and $\mathcal{L}_i$ is the location indicator for $\mathcal{G}_i$ within the molecular graph $\mathcal{G}$. $\mathcal{L}_i = (\mathcal{L}_i^{atom}, \mathcal{L}_i^{bond})$ consists of indices of $\mathcal{G}_i$'s atoms and bonds within the molecular graph $\mathcal{G}$, where $\mathcal{L}_i^{atom} = \{m | v_m \in \mathcal{V}_i\}$ and $\mathcal{L}_i^{bond} = \{(m,n) | (v_m, v_n) \in \mathcal{E}_i\}$.

This task emphasizes referential perception by mapping textual or conceptual references to their precise structural counterparts. It is analogous to object detection in vision and token-level alignment in NLP. Building upon CNER and BNSM, the new challenge imposed in RSL is the existence of multiple instances of the target and possible distractors. Those distractors are often with similar structures as the target, further challenging the low tolerance at fine grained level. Examples can be found in Figure 3.

Substructure Relationship Grounding (SRG): *Identify the relationships (e.g., composition, directed attachment, functional integration, or coexistence) between substructures within a molecule, as represented by a caption $\mathcal{X}$ and the corresponding molecular graph $\mathcal{G}$ as*

$$\begin{aligned} f_K : (\mathcal{X}, \mathcal{G}) &\mapsto \mathcal{K} \\ \mathcal{X} = \{x_i\},\ \mathcal{G} &= (\mathcal{V}, \mathcal{E}),\ \mathcal{G}_i, \mathcal{G}_j \subseteq \mathcal{G}, \\ \mathcal{K} &= \{k_{ij}\} \in \{\mathcal{G}_i\} \times \{\mathcal{G}_j\} \end{aligned} \tag{4}$$

where $\mathcal{G}_i$ and $\mathcal{G}_j$ are the ith and j^{th} substructure graphs, and k_{ij} is their identified relationship.

This task builds on referential perception by modeling the interactions and dependencies between molecular substructures, providing insights into their functional roles. It draws parallels to relation extraction in NLP and interaction modeling in molecular sciences. The key challenge in this task lies in the multidimensional nature of the relationships. Unlike conventional NLP relation extraction, which is primarily governed by semantic correlations between entities, SRG relationships are multidimensional, incorporating chemical, spatial, physical, and hierarchical factors. More specifically, this complexity means that chemical relationships, such as composition, directed attachment, or functional integration, are intricately intertwined with their associated physical factors. This contrasts sharply with NLP relations (e.g., is-a, is-part-of), which are often straightforwardly defined. Figure 4 illustrates this challenge.

Substructure Frequency Analysis (SFA): *Count the number of occurrences of a specified substructure (indicated by its name $n_i \in \mathcal{N}$) within the structural representation $\mathcal{G}$ of a given molecule as*

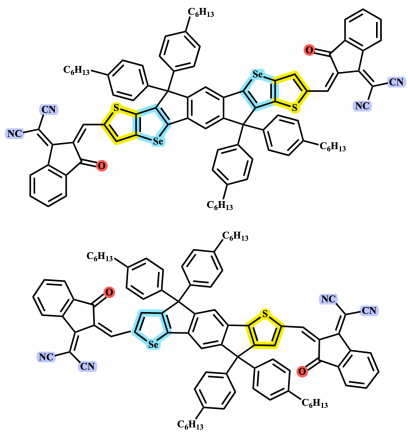

Figure 4: The relationship of "functional integration" between the *thiophene* (yellow) and *selenophene* (blue) rings varies significantly across different molecules (attached in one case but distinctly separate in another).

$$\begin{aligned} f_F : (\mathcal{N}, \mathcal{G}) &\mapsto \mathcal{F} \\ \mathcal{N} = \{N_i\},\ \mathcal{G} &= (\mathcal{V}, \mathcal{E}),\ \mathcal{G}_i \subseteq \mathcal{G}, \\ \mathcal{F} &= \{k_i\} \in \mathbb{N} \end{aligned} \tag{5}$$

where k_i is the frequency of n_i counted by the occurrences of its substructure graph $\mathcal{G}_i$ within $\mathcal{G}$.

This task extends referential perception by quantifying the presence of referenced substructures, supporting downstream molecular grounding tasks such as property prediction or functional analysis. It aligns with token frequency counting in NLP and motif detection in cheminformatics. However, this goes beyond a simple counting task. The complexity arising from multiple representation forms, hierarchical definitions, multidimensionality, and multiresolution makes the target of counting dynamic and context-dependent, unlike the fixed nature of token frequency analysis in NLP.

4 Benchmarking

Benchmarking in the chemical domain is expensive, largely due to its heavy reliance on human expertise. To build the largest molecular understanding benchmark to date, we adopt an interactive approach based on the Spiral Model (Boehm, 1986). Specifically, we develop a prototype of a grounding agent to facilitate the process. The agent automates data collection, cleaning, and structuring, after which the data is validated, corrected, or filtered by human experts. Data entries rejected by human experts are refined by the agent and resubmitted for further review. This iterative interaction

between humans and the agent continues until convergence is achieved. Throughout this process, the agent itself is iteratively improved as part of an exploration into effective grounding methodologies, while simultaneously enhancing both the scale and quality of the benchmark.

4.1 Grounding Agent Prototyping

Our study shows that the most effective approach is a multi-agent system composed of a meta-retriever, an LLM-based text interpreter, and a structure parser. The meta-retriever is built using PubChem APIs (Kim et al., 2024) and is responsible for collecting molecular names, properties, and descriptions. The text interpreter leverages large language models (LLMs) to perform named entity recognition and relationship analysis at the textual level. The structure parser is developed using RDKit[1] and handles structure retrieval, comparison, and validation.

These three agents work collaboratively: the meta-retriever gathers metadata as needed and provides it to the text interpreter as examples or contextual information for in-context learning. The text interpreter extracts names and relationships from captions, passing them to the structure parser, which converts the information into molecular structures. The structure parser then compares or validates the structures to produce grounded outputs. This process effectively handles all five grounding tasks.

4.2 Data Collection and Preprocessing

We collected molecules from existing molecular captioning datasets, such as ChEBI-20 (Edwards et al., 2021) and LPM-24 (Edwards et al., 2024). Additionally, we extended our collection with molecules published in chemical literature (Nagasawa et al.). In total, this resulted in a dataset of 55,989 molecules. The collected molecules exhibit varying levels of structural complexity. Specifically, the number of atoms per molecule ranges from 1 to 574, with a median value of 33. The number of rings varies from 0 to 69, while the number of bonds spans from 1 to 642.

For molecules lacking captions (approximately 2% of the dataset), we utilized GPT-4o (OpenAI et al., 2024) to generate detailed captions. This was achieved by inputting the molecule's IUPAC name, SMILES representation, relevant literature, and molecular structure image into GPT-4o, along with prompt templates designed by chemical experts (details provided in the Appendix A.1). The templates were tailored to generate substructure-focused content, such as identifying the substructures within a molecule, describing how they are connected, and outlining their properties. As a result, we constructed a dataset of 55,989 molecule-caption pairs.

4.3 Structurization and Annotation

The structuring and annotation process is performed iteratively, allowing our grounding agent to collaborate with human chemical experts. The 117k QA pairs listed in Table 1 are constructed based on the human annotation data. We split the QAs into training, validation, and testing sets using a split ratio (80%, 10%, 10%) on each task, and ensure that there is no overlapped molecule between different sets.

5 Experiments

5.1 Baselines

We employ 8 LLMs as baselines, including general-domain models like GPT4o (OpenAI et al., 2024) and LLaMA 3.1 (8B and 70B) (Grattafiori et al., 2024), as well as models specifically tailored for molecular understanding, such as Bio-T5+ (Pei et al., 2024), ChemLLM (7B) (Zhang et al., 2024a), and Mol-Instructions (Fang et al., 2024). Furthermore, we investigate LLM learning techniques, including In-Context Learning (ICL), such as Retrieval-Augmented Generation (RAG), and Supervised Fine-tuning (SFT) using LoRA (Hu et al., 2022). Given that molecular structures can be represented as graphs, we also incorporate Multimodal LLMs (MLLMs) like GPT4o Vision (OpenAI et al., 2024) and LLaVA-Next (Liu et al., 2023) in our evaluations.

5.2 Evaluation of Pretrained Models

Table 3 compares the performance of LLMs and MLLMs across five molecular grounding tasks. Overall, most tasks remain challenging for all baseline models, with accuracy generally below 0.5. In particular, BNSM, SFA, and RSL prove to be the most difficult, with all models achieving accuracies below 0.337. By contrast, CNER and SRG exhibit relatively better performance. The highest F1-score for CNER is 0.633 and the highest accuracy for SRG is 0.803, which are achieved by GPT-4o. For the CNER task, models often

[1] RDKit: Open-source cheminformatics, https://www.rdkit.org

	Tasks	CNER	BNSM	SRG	SFA	S-RSL			M-RSL			
	Metric	F1	Acc.	F1	Acc.	$F1_l$	IoU_l	Acc_g	$F1_l$	IoU_l	Acc_g	Cov_s
LLM	GPT-4o	**0.633**	0.125	**0.160**	**0.337**	0.015	0.148	**0.755**	**0.011**	**0.073**	**0.429**	**0.543**
	LLaMA 3.1-8B	0.504	0.092	0.001	0.111	0.006	**0.175**	0.672	0.000	0.018	0.083	0.126
	LLaMA 3.1-70B	0.637	0.063	0.004	0.233	0.008	0.100	0.473	0.001	0.009	0.031	0.045
	BioT5+	0.000	0.000	0.000	0.000	0.000	0.000	0.000	0.000	0.000	0.000	0.000
	ChemLLM-7B	0.000	0.000	0.000	0.154	0.000	0.000	0.678	0.000	0.000	0.000	0.000
	Mol-Instructions	0.152	0.000	0.000	0.000	0.000	0.000	0.000	0.000	0.000	0.000	0.000
MLLM	GPT-4o-Vision	0.578	**0.246**	0.061	0.321	0.004	0.052	0.332	0.000	0.001	0.012	0.016
	LLaVA-Next-7B	0.412	0.021	0.042	0.142	**0.020**	0.174	0.737	0.000	0.001	0.004	0.005

Table 3: Comparison of LLMs and MLLMs performance across five molecular grounding tasks. For RSL, results are reported at both singular (S-RSL) and multiple (M-RSL) substructure levels.

	Tasks	CNER	BNSM	SRG	SFA	S-RSL	M-RSL
	Metric	F1	Acc.	F1	Acc.	$F1_l$	$F1_l$
Baselines	GPT-4o	0.633	0.125	0.160	0.337	0.015	0.011
	LLaMA 3.1-8B	0.504	0.092	0.001	0.111	0.006	0.000
	Mol-Instructions	0.152	0.000	0.000	0.001	0.000	0.000
Baselines + ICL (Few-shot)	GPT-4o	0.721	0.314	**0.385**	0.754	0.017	0.270
	LLaMA 3.1-8B	0.722	0.180	0.195	0.587	0.003	0.120
	Mol-Instructions	0.350	0.000	0.000	0.117	0.000	0.036
Baselines + ICL (RAG)	GPT-4o	**0.915**	0.397	0.368	0.754	0.174	0.171
	LLaMA 3.1-8B	0.881	0.361	0.072	0.655	0.149	0.113
	Mol-Instructions	0.864	0.083	0.000	0.561	0.091	0.072
Baselines + SFT	LLaMA 3.1-8B	0.641	**0.426**	0.078	0.899	0.275	0.315
	Mol-Instructions	0.727	0.397	0.072	**0.917**	**0.295**	**0.337**

Table 4: Performance improvement through the integration of ICL and SFT techniques across five grounding tasks. For RSL, results are presented at both singular (S-RSL) and multiple (M-RSL) substructure levels.

over-extract functionality words as chemical substructure names (e.g., "amide functionality") and struggle to correctly assign roles to extracted chemical names. For the SFA, models perform well on counting non-existent rings but struggle with monocyclic ring identification due to subtle structural differences. For example, the predicted probabilities of the benzene to be a donor or acceptor is Moreover, BioT5+ fails to follow instructions, and Mol-Instructions exhibits a strong bias in selecting question choices . While chemical name recognition (CNER) is relatively well-handled, with most models achieving an F1-score above 0.9, smaller models (e.g., LLaMA 3.1-8B, ChemLLM-7B) similar names (e.g., *ether* vs. *ester*) For more complex tasks (BNSM and SRG), performance remains low, even for the best model, GPT-4o, which achieves only 0.125 and 0.333 accuracy, respectively. In BNSM, models perform well for simple structures but struggle with complex mappings, often generating incorrect yet structurally similar names or SMILES strings. SRG results indicate difficulty in establishing substructures' relationships, with models misinterpreting textual cues and neglecting structural connections. RSL task witnessed a particularly poor performance, with the best F1 (0.020) and IoU (0.174). In singular RSL, GPT-4o achieves the highest accuracy (0.755) but with low IoU (0.148), while LLaMA 3.1-8B prioritizes broader highlighting at the cost of accuracy. For multiple RSL, most models generate invalid outputs and show low substructure coverage (max 54.3%). MLLMs, despite access to structural images, do not surpass LLMs (except BNSM).

5.3 Evaluation of ICL and SFT

Table 4 examines how ICL and SFT impact the tasks. Overall, while both ICL and SFT improve results, the gains in RSL tasks remain limited. ICL significantly enhances tasks requiring chemical knowledge recall, particularly CNER and SFA. Few-shot learning boosts GPT-4o and LLaMA 3.1-8B accuracy to 99.4% and 96.0% on CNER, respectively. RAG dramatically improves SFA performance, with increases of 124% for GPT-4o and 489% for LLaMA 3.1-8B. Mol-Instructions sees an extreme gain of 56009%, though this may indicate prior poor performance rather than true capability improvement. SFT provides the most substantial boost for grounding tasks. For instance, LLaMA 3.1-8B's F1-score in singular RSL gains from 0.006 to 0.275, and in multiple RSL from 0.001 to 0.315.

	Tasks	S-RSL				M-RSL				
	Metic	$F1_l$	IoU_l	IoU_g	Acc_g	$F1_l$	IoU_l	IoU_g	Acc_g	Cov_s
Pre-trained	GPT-4o	0.015	0.148	0.135	0.755	0.011	0.073	0.054	0.429	0.543
	LLaMA 3.1-8B	0.006	0.175	0.141	0.672	0.000	0.018	0.018	0.083	0.126
	Mol-Instruct-8B	0.000	0.000	0.000	0.000	0.000	0.000	0.000	0.000	0.000
ICL(Few-shot)	GPT4o	0.017	0.059	0.143	0.291	0.270	0.454	0.399	**0.779**	**0.905**
	LLaMA 3.1-8B	0.003	0.014	0.052	0.102	0.120	0.207	0.181	0.379	0.432
	Mol-Instruct-8B	0.000	0.000	0.000	0.000	0.036	0.079	0.049	0.117	0.143
ICL(RAG)	GPT4o	0.174	0.361	0.337	0.415	0.171	0.301	0.290	0.369	0.718
	LLaMA 3.1-8B	0.149	0.332	0.307	0.387	0.113	0.262	0.255	0.344	0.760
	Mol-Instruct-8B	0.091	0.284	0.243	0.326	0.072	0.203	0.183	0.256	0.637
SFT	LLaMA 3.1-8B	0.275	0.483	0.466	0.548	0.315	0.515	0.487	0.587	0.850
	Mol-Instruct-8B	0.295	0.499	0.486	0.565	0.337	0.518	0.493	0.586	0.833
MLLM	GPT4o	0.004	0.052	0.054	0.332	0.000	0.001	0.001	0.012	0.016
	LLaVA-Next-7B	0.020	0.174	0.112	0.737	0.000	0.001	0.001	0.004	0.005
	LLaMA 3.2-11B-Vision	0.010	0.113	0.085	0.555	0.003	0.062	0.046	0.280	0.402
Grounding Agent	GPT4o	**0.630**	**0.685**	**0.647**	**0.933**	**0.541**	**0.566**	**0.546**	0.776	0.818
	LLaMA 3.1-8B	0.334	0.383	0.364	0.863	0.426	0.527	0.448	0.580	0.688
	Mol-Instruct-8B	0.000	0.000	0.000	0.000	0.311	0.446	0.310	0.356	0.382

Table 5: Performance of grounding agents with different backbones. Both local ($_l$) and global ($_g$) RSL are reported.

Mol-Instructions follows a similar trend, demonstrating SFT's effectiveness in refining molecular representations. However, improvements are not consistent across models. ICL techniques sometimes degrade performance. For example, Few-shot learning and RAG lower GPT-4o's accuracy on SRG, as additional examples introduce substructure relationships that distract the model.

5.4 Evaluation of the Agent Prototype

Table 5 compares RSL performance of the agents and other models. The grounding agents outperform other models in singular and multiple RSL tasks across most metrics, except for substructure coverage. Their advantage primarily stems from an additional sub-graph matching tool, which enables better structure generation for queried chemical entities, leading to more accurate grounding. However, grounding agents still exhibit limitations. One key weakness is name-to-structure mapping, where small LLMs like LLaMA 3.1-8B achieve low accuracy (37.9%). Additionally, agents sometimes match results across different substructures and struggle to filter out irrelevant grounding results based on context. Figures 5 and 6 visualizes these issues. Figure 5 shows the grounding result for *benzene*. While GPT-4o identifies correctly that *benzene* is a six-membered substructure, its atom indices are scattered across multiple substructures. The grounding agent provides more accurate results but fails to fit the constraints that *Fluorine* substituents described in the caption. Another example in Figure 6 is to show a drawback of using subgraph retrieval technique for RSL where locations are overlapped generated for a chain and are scattered across different substructures.

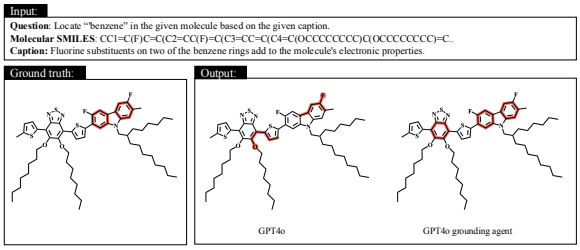

Figure 5: Comparison of the ground truth and grounding outputs by GPT4o and the grounding agent.

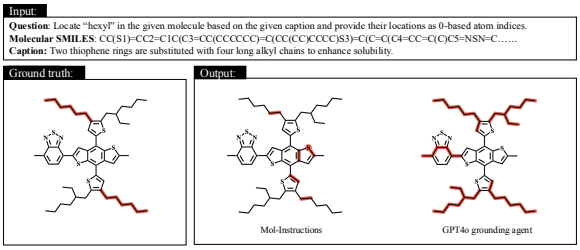

Figure 6: Irrelevant and wrong grounding results generated by Mol-Instructions and the grounding agent.

5.5 Can Ground Help Downstream Tasks?

We conducted experiments to evaluate the impact of molecular grounding on molecular captioning and classification. For molecular captioning, we incorporate grounding results generated by the grounding agent (GPT4-based) as additional input. As shown in Table 6, this additional information improved performance across all BLEU metrics.

Model	BLEU1	BLEU2	BLEU3	BLEU4
GPT4o	30.861	15.683	8.032	4.199
+ Grounding	**31.178**	**16.698**	**9.002**	**5.004**

Table 6: Performance on Molecular Captioning

Model	Aim.	Cov.	Acc.	Abs.T	Abs.F
ATC-CNN	67.86	66.65	65.04	60.65	**3.83**
+ Grounding	**70.15**	**71.71**	**67.81**	**61.49**	4.18

Table 7: Performance Comparison on Molecular Classification Task. Note that lower Abs.F is better.

For molecular classification, we investigated the effectiveness of integrating molecular substructure information into ATC classification (Anatomical, Therapeutic, Chemical). We use ATC-CNN (Cao et al., 2022) as the baseline and conduct the experiments on ATC-SMILES (Cao et al., 2022) dataset with the resulting substructures. As shown in Table 7, incorporating substructure information led to significant performance gains across almost all evaluation metrics, including aiming (+3.37%), coverage (+7.59%), accuracy (+4.26%), and absolute true (+1.38%), demonstrating that molecular grounding enhances drug classification.

6 Conclusion

This paper has introduced a molecular grounding benchmark to enhance the referential aspect of molecular understanding. MolGround, with 117k QA pairs across five subtasks, is the largest molecular QA benchmark. Our evaluation shows that existing LLMs struggle with these tasks, with SFT and ICL yielding minor improvements. Our grounding prototype outperforms existing models and enhances downstream tasks like captioning and ATC classification.

References

Yuzuki Arai and Sho Tsugawa. 2024. Do large language models defend inferentialist semantics?: On the logical expressivism and anti-representationalism of llms. *arXiv preprint arXiv:2412.14501*.

B Boehm. 1986. A spiral model of software development and enhancement. *SIGSOFT Softw. Eng. Notes*, 11(4):14–24.

Yi Cao, Zhen-Qun Yang, Xu-Lu Zhang, Wenqi Fan, Yaowei Wang, Jiajun Shen, Dong-Qing Wei, Qing Li, and Xiao-Yong Wei. 2022. Identifying the kind behind smiles—anatomical therapeutic chemical classification using structure-only representations. *Briefings in Bioinformatics*, 23(5):bbac346.

Nino B Cocchiarella. 1974. Fregean semantics for a realist ontology. *Notre Dame Journal of Formal Logic*, 15(4):552–568.

Jiajun Deng, Zhengyuan Yang, Tianlang Chen, Wengang Zhou, and Houqiang Li. 2021. Transvg: End-to-end visual grounding with transformers. In *Proceedings of the IEEE/CVF International Conference on Computer Vision (ICCV)*, pages 1769–1779.

Yuheng Ding, Bo Qiang, Qixuan Chen, Yiqiao Liu, Liangren Zhang, and Zhenming Liu. 2024. Exploring chemical reaction space with machine learning models: Representation and feature perspective. *Journal of Chemical Information and Modeling*, 64(8):2955–2970.

Carl Edwards, Qingyun Wang, Lawrence Zhao, and Heng Ji. 2024. L+M-24: Building a dataset for Language+Molecules @ ACL 2024. In *Proceedings of the 1st Workshop on Language + Molecules (L+M 2024)*, pages 1–9.

Carl Edwards, ChengXiang Zhai, and Heng Ji. 2021. Text2Mol: Cross-modal molecule retrieval with natural language queries. In *Proceedings of the 2021 Conference on Empirical Methods in Natural Language Processing*, pages 595–607.

Lei Fang, Junren Li, Ming Zhao, Li Tan, and Jian-Guang Lou. 2022a. Single-step retrosynthesis prediction by leveraging commonly preserved substructures. *Nature Communications*, 14.

Xiaomin Fang, Lihang Liu, Jieqiong Lei, Donglong He, Shanzhuo Zhang, Jingbo Zhou, Fan Wang, Hua Wu, and Haifeng Wang. 2022b. Geometry-enhanced molecular representation learning for property prediction. *Nature Machine Intelligence*, 4:127–134.

Yin Fang, Xiaozhuan Liang, Ningyu Zhang, Kangwei Liu, Rui Huang, Zhuo Chen, Xiaohui Fan, and Huajun Chen. 2024. Mol-instructions: A large-scale biomolecular instruction dataset for large language models. In *The Twelfth International Conference on Learning Representations*.

David Fooshee, Aaron Mood, Eugene Gutman, Mohammadamin Tavakoli, Gregor Urban, Frances Liu, Nancy Huynh, David Van Vranken, and Pierre Baldi. 2018. Deep learning for chemical reaction prediction. *Molecular Systems Design and Engineering*, 3:442–452.

Lei Gao and Ling Guan. 2023. Interpretability of machine learning: Recent advances and future prospects. *IEEE MultiMedia*, 30(4):105–118.

Peter T Geach. 1950. Russell's theory of descriptions. *Analysis*, 10(4):84–88.

Aaron Grattafiori, Abhimanyu Dubey, Abhinav Jauhri, Abhinav Pandey, Abhishek Kadian, Ahmad Al-Dahle, Aiesha Letman, Akhil Mathur, Alan Schelten, Alex Vaughan, Amy Yang, Angela Fan, Anirudh

Goyal, Anthony Hartshorn, Aobo Yang, Archi Mitra, Archie Sravankumar, Artem Korenev, Arthur Hinsvark, Arun Rao, Aston Zhang, Aurelien Rodriguez, Austen Gregerson, Ava Spataru, Baptiste Roziere, Bethany Biron, Binh Tang, Bobbie Chern, Charlotte Caucheteux, Chaya Nayak, Chloe Bi, Chris Marra, Chris McConnell, Christian Keller, Christophe Touret, Chunyang Wu, Corinne Wong, Cristian Canton Ferrer, Cyrus Nikolaidis, Damien Allonsius, Daniel Song, Danielle Pintz, Danny Livshits, Danny Wyatt, David Esiobu, Dhruv Choudhary, Dhruv Mahajan, Diego Garcia-Olano, Diego Perino, Dieuwke Hupkes, Egor Lakomkin, Ehab AlBadawy, Elina Lobanova, Emily Dinan, Eric Michael Smith, Filip Radenovic, Francisco Guzmán, Frank Zhang, Gabriel Synnaeve, Gabrielle Lee, Georgia Lewis Anderson, Govind Thattai, Graeme Nail, Gregoire Mialon, Guan Pang, Guillem Cucurell, Hailey Nguyen, Hannah Korevaar, Hu Xu, Hugo Touvron, Iliyan Zarov, Imanol Arrieta Ibarra, Isabel Kloumann, Ishan Misra, Ivan Evtimov, Jack Zhang, Jade Copet, Jaewon Lee, Jan Geffert, Jana Vranes, Jason Park, Jay Mahadeokar, Jeet Shah, Jelmer van der Linde, Jennifer Billock, Jenny Hong, Jenya Lee, Jeremy Fu, Jianfeng Chi, Jianyu Huang, Jiawen Liu, Jie Wang, Jiecao Yu, Joanna Bitton, Joe Spisak, Jongsoo Park, Joseph Rocca, Joshua Johnstun, Joshua Saxe, Junteng Jia, Kalyan Vasuden Alwala, Karthik Prasad, Kartikeya Upasani, Kate Plawiak, Ke Li, Kenneth Heafield, Kevin Stone, Khalid El-Arini, Krithika Iyer, Kshitiz Malik, Kuenley Chiu, Kunal Bhalla, Kushal Lakhotia, Lauren Rantala-Yeary, Laurens van der Maaten, Lawrence Chen, Liang Tan, Liz Jenkins, Louis Martin, Lovish Madaan, Lubo Malo, Lukas Blecher, Lukas Landzaat, Luke de Oliveira, Madeline Muzzi, Mahesh Pasupuleti, Mannat Singh, Manohar Paluri, Marcin Kardas, Maria Tsimpoukelli, Mathew Oldham, Mathieu Rita, Maya Pavlova, Melanie Kambadur, Mike Lewis, Min Si, Mitesh Kumar Singh, Mona Hassan, Naman Goyal, Narjes Torabi, Nikolay Bashlykov, Nikolay Bogoychev, Niladri Chatterji, Ning Zhang, Olivier Duchenne, Onur Çelebi, Patrick Alrassy, Pengchuan Zhang, Pengwei Li, Petar Vasic, Peter Weng, Prajjwal Bhargava, Pratik Dubal, Praveen Krishnan, Punit Singh Koura, Puxin Xu, Qing He, Qingxiao Dong, Ragavan Srinivasan, Raj Ganapathy, Ramon Calderer, Ricardo Silveira Cabral, Robert Stojnic, Roberta Raileanu, Rohan Maheswari, Rohit Girdhar, Rohit Patel, Romain Sauvestre, Ronnie Polidoro, Roshan Sumbaly, Ross Taylor, Ruan Silva, Rui Hou, Rui Wang, Saghar Hosseini, Sahana Chennabasappa, Sanjay Singh, Sean Bell, Seohyun Sonia Kim, Sergey Edunov, Shaoliang Nie, Sharan Narang, Sharath Raparthy, Sheng Shen, Shengye Wan, Shruti Bhosale, Shun Zhang, Simon Vandenhende, Soumya Batra, Spencer Whitman, Sten Sootla, Stephane Collot, Suchin Gururangan, Sydney Borodinsky, Tamar Herman, Tara Fowler, Tarek Sheasha, Thomas Georgiou, Thomas Scialom, Tobias Speckbacher, Todor Mihaylov, Tong Xiao, Ujjwal Karn, Vedanuj Goswami, Vibhor Gupta, Vignesh Ramanathan, Viktor Kerkez, Vincent Gonguet, Virginie Do, Vish Vogeti, Vítor Albiero, Vladan Petrovic, Weiwei Chu, Wenhan Xiong, Wenyin Fu, Whitney Meers, Xavier Martinet, Xiaodong Wang, Xiaofang Wang, Xiaoqing Ellen Tan, Xide Xia, Xinfeng Xie, Xuchao Jia, Xuewei Wang, Yaelle Goldschlag, Yashesh Gaur, Yasmine Babaei, Yi Wen, Yiwen Song, Yuchen Zhang, Yue Li, Yuning Mao, Zacharie Delpierre Coudert, Zheng Yan, Zhengxing Chen, Zoe Papakipos, Aaditya Singh, Aayushi Srivastava, Abha Jain, Adam Kelsey, Adam Shajnfeld, Adithya Gangidi, Adolfo Victoria, Ahuva Goldstand, Ajay Menon, Ajay Sharma, Alex Boesenberg, Alexei Baevski, Allie Feinstein, Amanda Kallet, Amit Sangani, Amos Teo, Anam Yunus, Andrei Lupu, Andres Alvarado, Andrew Caples, Andrew Gu, Andrew Ho, Andrew Poulton, Andrew Ryan, Ankit Ramchandani, Annie Dong, Annie Franco, Anuj Goyal, Aparajita Saraf, Arkabandhu Chowdhury, Ashley Gabriel, Ashwin Bharambe, Assaf Eisenman, Azadeh Yazdan, Beau James, Ben Maurer, Benjamin Leonhardi, Bernie Huang, Beth Loyd, Beto De Paola, Bhargavi Paranjape, Bing Liu, Bo Wu, Boyu Ni, Braden Hancock, Bram Wasti, Brandon Spence, Brani Stojkovic, Brian Gamido, Britt Montalvo, Carl Parker, Carly Burton, Catalina Mejia, Ce Liu, Changhan Wang, Changkyu Kim, Chao Zhou, Chester Hu, Ching-Hsiang Chu, Chris Cai, Chris Tindal, Christoph Feichtenhofer, Cynthia Gao, Damon Civin, Dana Beaty, Daniel Kreymer, Daniel Li, David Adkins, David Xu, Davide Testuggine, Delia David, Devi Parikh, Diana Liskovich, Didem Foss, Dingkang Wang, Duc Le, Dustin Holland, Edward Dowling, Eissa Jamil, Elaine Montgomery, Eleonora Presani, Emily Hahn, Emily Wood, Eric-Tuan Le, Erik Brinkman, Esteban Arcaute, Evan Dunbar, Evan Smothers, Fei Sun, Felix Kreuk, Feng Tian, Filippos Kokkinos, Firat Ozgenel, Francesco Caggioni, Frank Kanayet, Frank Seide, Gabriela Medina Florez, Gabriella Schwarz, Gada Badeer, Georgia Swee, Gil Halpern, Grant Herman, Grigory Sizov, Guangyi, Zhang, Guna Lakshminarayanan, Hakan Inan, Hamid Shojanazeri, Han Zou, Hannah Wang, Hanwen Zha, Haroun Habeeb, Harrison Rudolph, Helen Suk, Henry Aspegren, Hunter Goldman, Hongyuan Zhan, Ibrahim Damlaj, Igor Molybog, Igor Tufanov, Ilias Leontiadis, Irina-Elena Veliche, Itai Gat, Jake Weissman, James Geboski, James Kohli, Janice Lam, Japhet Asher, Jean-Baptiste Gaya, Jeff Marcus, Jeff Tang, Jennifer Chan, Jenny Zhen, Jeremy Reizenstein, Jeremy Teboul, Jessica Zhong, Jian Jin, Jingyi Yang, Joe Cummings, Jon Carvill, Jon Shepard, Jonathan McPhie, Jonathan Torres, Josh Ginsburg, Junjie Wang, Kai Wu, Kam Hou U, Karan Saxena, Kartikay Khandelwal, Katayoun Zand, Kathy Matosich, Kaushik Veeraraghavan, Kelly Michelena, Keqian Li, Kiran Jagadeesh, Kun Huang, Kunal Chawla, Kyle Huang, Lailin Chen, Lakshya Garg, Lavender A, Leandro Silva, Lee Bell, Lei Zhang, Liangpeng Guo, Licheng Yu, Liron Moshkovich, Luca Wehrstedt, Madian Khabsa, Manav Avalani, Manish Bhatt, Martynas Mankus, Matan Hasson, Matthew Lennie, Matthias Reso, Maxim Groshev, Maxim Naumov, Maya Lathi, Meghan Keneally, Miao Liu, Michael L. Seltzer, Michal Valko, Michelle Restrepo, Mihir Patel, Mik Vyatskov, Mikayel Samvelyan, Mike Clark, Mike Macey, Mike Wang, Miquel Jubert Hermoso,

Mo Metanat, Mohammad Rastegari, Munish Bansal, Nandhini Santhanam, Natascha Parks, Natasha White, Navyata Bawa, Nayan Singhal, Nick Egebo, Nicolas Usunier, Nikhil Mehta, Nikolay Pavlovich Laptev, Ning Dong, Norman Cheng, Oleg Chernoguz, Olivia Hart, Omkar Salpekar, Ozlem Kalinli, Parkin Kent, Parth Parekh, Paul Saab, Pavan Balaji, Pedro Rittner, Philip Bontrager, Pierre Roux, Piotr Dollar, Polina Zvyagina, Prashant Ratanchandani, Pritish Yuvraj, Qian Liang, Rachad Alao, Rachel Rodriguez, Rafi Ayub, Raghotham Murthy, Raghu Nayani, Rahul Mitra, Rangaprabhu Parthasarathy, Raymond Li, Rebekkah Hogan, Robin Battey, Rocky Wang, Russ Howes, Ruty Rinott, Sachin Mehta, Sachin Siby, Sai Jayesh Bondu, Samyak Datta, Sara Chugh, Sara Hunt, Sargun Dhillon, Sasha Sidorov, Satadru Pan, Saurabh Mahajan, Saurabh Verma, Seiji Yamamoto, Sharadh Ramaswamy, Shaun Lindsay, Shaun Lindsay, Sheng Feng, Shenghao Lin, Shengxin Cindy Zha, Shishir Patil, Shiva Shankar, Shuqiang Zhang, Shuqiang Zhang, Sinong Wang, Sneha Agarwal, Soji Sajuyigbe, Soumith Chintala, Stephanie Max, Stephen Chen, Steve Kehoe, Steve Satterfield, Sudarshan Govindaprasad, Sumit Gupta, Summer Deng, Sungmin Cho, Sunny Virk, Suraj Subramanian, Sy Choudhury, Sydney Goldman, Tal Remez, Tamar Glaser, Tamara Best, Thilo Koehler, Thomas Robinson, Tianhe Li, Tianjun Zhang, Tim Matthews, Timothy Chou, Tzook Shaked, Varun Vontimitta, Victoria Ajayi, Victoria Montanez, Vijai Mohan, Vinay Satish Kumar, Vishal Mangla, Vlad Ionescu, Vlad Poenaru, Vlad Tiberiu Mihailescu, Vladimir Ivanov, Wei Li, Wenchen Wang, Wenwen Jiang, Wes Bouaziz, Will Constable, Xiaocheng Tang, Xiaojian Wu, Xiaolan Wang, Xilun Wu, Xinbo Gao, Yaniv Kleinman, Yanjun Chen, Ye Hu, Ye Jia, Ye Qi, Yenda Li, Yilin Zhang, Ying Zhang, Yossi Adi, Youngjin Nam, Yu, Wang, Yu Zhao, Yuchen Hao, Yundi Qian, Yunlu Li, Yuzi He, Zach Rait, Zachary DeVito, Zef Rosnbrick, Zhaoduo Wen, Zhenyu Yang, Zhiwei Zhao, and Zhiyu Ma. 2024. The llama 3 herd of models. *Preprint*, arXiv:2407.21783.

Marti A. Hearst, Susan T Dumais, Edgar Osuna, John Platt, and Bernhard Scholkopf. 1998. Support vector machines. *IEEE Intelligent Systems and their applications*, 13(4):18–28.

David W Hosmer Jr, Stanley Lemeshow, and Rodney X Sturdivant. 2013. *Applied logistic regression*. John Wiley & Sons.

Edward J Hu, Yelong Shen, Phillip Wallis, Zeyuan Allen-Zhu, Yuanzhi Li, Shean Wang, Lu Wang, and Weizhu Chen. 2022. LoRA: Low-rank adaptation of large language models. In *International Conference on Learning Representations*.

Chenqing Hua, Sitao Luan, Minkai Xu, Zhitao Ying, Jie Fu, Stefano Ermon, and Doina Precup. 2024. Mudiff: Unified diffusion for complete molecule generation. In *Learning on Graphs Conference*, pages 33–1. PMLR.

Richard Janissen, Roman Barth, Minco Polinder, Jaco van der Torre, and Cees Dekker. 2024. Single-molecule visualization of twin-supercoiled domains generated during transcription. *Nucleic acids research*, 52(4):1677–1687.

Richard Evans John Jumper, Alexander Pritzel, Tim Green, Michael Figurnov, Olaf Ronneberger, Kathryn Tunyasuvunakool, Russ Bates, Augustin Žídek, Anna Potapenko, Alex Bridgland, Clemens Meyer, Simon A. A. Kohl, Andrew J. Ballard, Andrew Cowie, Bernardino Romera-Paredes, Stanislav Nikolov, Rishub Jain, Jonas Adler, Trevor Back, Stig Petersen, David Reiman, Ellen Clancy, Michal Zielinski, Martin Steinegger, Michalina Pacholska, Tamas Berghammer, Sebastian Bodenstein, David Silver, Oriol Vinyals, Andrew W. Senior, Koray Kavukcuoglu, Pushmeet Kohli, and Demis Hassabis. 2021. Highly accurate protein structure prediction with alphafold. *Nature*, 596:583–589.

Hans Kamp and Uwe Reyle. 1993. From discourse to logic - introduction to modeltheoretic semantics of natural language, formal logic and discourse representation theory. In *Studies in Linguistics and Philosophy*.

Sunghwan Kim, Jie Chen, Tiejun Cheng, Asta Gindulyte, Jia He, Siqian He, Qingliang Li, Benjamin A Shoemaker, Paul A Thiessen, Bo Yu, Leonid Zaslavsky, Jian Zhang, and Evan E Bolton. 2024. Pubchem 2025 update. *Nucleic Acids Research*, 53(D1):D1516–D1525.

Pat Langley, Wayne Iba, Kevin Thompson, et al. 1992. An analysis of bayesian classifiers. In *Aaai*, volume 90, pages 223–228. Citeseer.

Jiatong Li, Yunqing Liu, Wenqi Fan, Xiao-Yong Wei, Hui Liu, Jiliang Tang, and Qing Li. 2024. Empowering Molecule Discovery for Molecule-Caption Translation With Large Language Models: A ChatGPT Perspective . *IEEE Transactions on Knowledge & Data Engineering*, 36(11):6071–6083.

Christopher A. Lipinski, Franco Lombardo, Beryl W. Dominy, and Paul J. Feeney. 1997. Experimental and computational approaches to estimate solubility and permeability in drug discovery and development settings. *Advanced Drug Delivery Reviews*, 23(1):3–25.

Haotian Liu, Chunyuan Li, Qingyang Wu, and Yong Jae Lee. 2023. Visual instruction tuning.

Xingyu Lu, He Cao, Zijing Liu, Shengyuan Bai, Leqing Chen, Yuan Yao, Hai-Tao Zheng, and Yu Li. 2024. MoleculeQA: A dataset to evaluate factual accuracy in molecular comprehension. In *Findings of the Association for Computational Linguistics: EMNLP 2024*, pages 3769–3789.

Tianren Ma, Lingxi Xie, Yunjie Tian, Boyu Yang, Yuan Zhang, David Doermann, and Qixiang Ye. 2024. Clawmachine: Fetching visual tokens as an

entity for referring and grounding. *arXiv preprint arXiv:2406.11327*.

Shinji Nagasawa, Eman Al-Naamani, and Akinori Saeki. Computer-aided screening of conjugated polymers for organic solar cell: Classification by random forest. 9(10):2639–2646. Publisher: American Chemical Society.

OpenAI, Josh Achiam, Steven Adler, Sandhini Agarwal, Lama Ahmad, Ilge Akkaya, Florencia Leoni Aleman, Diogo Almeida, Janko Altenschmidt, Sam Altman, Shyamal Anadkat, Red Avila, Igor Babuschkin, Suchir Balaji, Valerie Balcom, Paul Baltescu, Haiming Bao, Mohammad Bavarian, Jeff Belgum, Irwan Bello, Jake Berdine, Gabriel Bernadett-Shapiro, Christopher Berner, Lenny Bogdonoff, Oleg Boiko, Madelaine Boyd, Anna-Luisa Brakman, Greg Brockman, Tim Brooks, Miles Brundage, Kevin Button, Trevor Cai, Rosie Campbell, Andrew Cann, Brittany Carey, Chelsea Carlson, Rory Carmichael, Brooke Chan, Che Chang, Fotis Chantzis, Derek Chen, Sully Chen, Ruby Chen, Jason Chen, Mark Chen, Ben Chess, Chester Cho, Casey Chu, Hyung Won Chung, Dave Cummings, Jeremiah Currier, Yunxing Dai, Cory Decareaux, Thomas Degry, Noah Deutsch, Damien Deville, Arka Dhar, David Dohan, Steve Dowling, Sheila Dunning, Adrien Ecoffet, Atty Eleti, Tyna Eloundou, David Farhi, Liam Fedus, Niko Felix, Simón Posada Fishman, Juston Forte, Isabella Fulford, Leo Gao, Elie Georges, Christian Gibson, Vik Goel, Tarun Gogineni, Gabriel Goh, Rapha Gontijo-Lopes, Jonathan Gordon, Morgan Grafstein, Scott Gray, Ryan Greene, Joshua Gross, Shixiang Shane Gu, Yufei Guo, Chris Hallacy, Jesse Han, Jeff Harris, Yuchen He, Mike Heaton, Johannes Heidecke, Chris Hesse, Alan Hickey, Wade Hickey, Peter Hoeschele, Brandon Houghton, Kenny Hsu, Shengli Hu, Xin Hu, Joost Huizinga, Shantanu Jain, Shawn Jain, Joanne Jang, Angela Jiang, Roger Jiang, Haozhun Jin, Denny Jin, Shino Jomoto, Billie Jonn, Heewoo Jun, Tomer Kaftan, Łukasz Kaiser, Ali Kamali, Ingmar Kanitscheider, Nitish Shirish Keskar, Tabarak Khan, Logan Kilpatrick, Jong Wook Kim, Christina Kim, Yongjik Kim, Jan Hendrik Kirchner, Jamie Kiros, Matt Knight, Daniel Kokotajlo, Łukasz Kondraciuk, Andrew Kondrich, Aris Konstantinidis, Kyle Kosic, Gretchen Krueger, Vishal Kuo, Michael Lampe, Ikai Lan, Teddy Lee, Jan Leike, Jade Leung, Daniel Levy, Chak Ming Li, Rachel Lim, Molly Lin, Stephanie Lin, Mateusz Litwin, Theresa Lopez, Ryan Lowe, Patricia Lue, Anna Makanju, Kim Malfacini, Sam Manning, Todor Markov, Yaniv Markovski, Bianca Martin, Katie Mayer, Andrew Mayne, Bob McGrew, Scott Mayer McKinney, Christine McLeavey, Paul McMillan, Jake McNeil, David Medina, Aalok Mehta, Jacob Menick, Luke Metz, Andrey Mishchenko, Pamela Mishkin, Vinnie Monaco, Evan Morikawa, Daniel Mossing, Tong Mu, Mira Murati, Oleg Murk, David Mély, Ashvin Nair, Reiichiro Nakano, Rajeev Nayak, Arvind Neelakantan, Richard Ngo, Hyeonwoo Noh, Long Ouyang, Cullen O'Keefe, Jakub Pachocki, Alex Paino, Joe Palermo, Ashley Pantuliano, Giambattista Parascandolo, Joel Parish, Emy Parparita, Alex Passos, Mikhail Pavlov, Andrew Peng, Adam Perelman, Filipe de Avila Belbute Peres, Michael Petrov, Henrique Ponde de Oliveira Pinto, Michael, Pokorny, Michelle Pokrass, Vitchyr H. Pong, Tolly Powell, Alethea Power, Boris Power, Elizabeth Proehl, Raul Puri, Alec Radford, Jack Rae, Aditya Ramesh, Cameron Raymond, Francis Real, Kendra Rimbach, Carl Ross, Bob Rotsted, Henri Roussez, Nick Ryder, Mario Saltarelli, Ted Sanders, Shibani Santurkar, Girish Sastry, Heather Schmidt, David Schnurr, John Schulman, Daniel Selsam, Kyla Sheppard, Toki Sherbakov, Jessica Shieh, Sarah Shoker, Pranav Shyam, Szymon Sidor, Eric Sigler, Maddie Simens, Jordan Sitkin, Katarina Slama, Ian Sohl, Benjamin Sokolowsky, Yang Song, Natalie Staudacher, Felipe Petroski Such, Natalie Summers, Ilya Sutskever, Jie Tang, Nikolas Tezak, Madeleine B. Thompson, Phil Tillet, Amin Tootoonchian, Elizabeth Tseng, Preston Tuggle, Nick Turley, Jerry Tworek, Juan Felipe Cerón Uribe, Andrea Vallone, Arun Vijayvergiya, Chelsea Voss, Carroll Wainwright, Justin Jay Wang, Alvin Wang, Ben Wang, Jonathan Ward, Jason Wei, CJ Weinmann, Akila Welihinda, Peter Welinder, Jiayi Weng, Lilian Weng, Matt Wiethoff, Dave Willner, Clemens Winter, Samuel Wolrich, Hannah Wong, Lauren Workman, Sherwin Wu, Jeff Wu, Michael Wu, Kai Xiao, Tao Xu, Sarah Yoo, Kevin Yu, Qiming Yuan, Wojciech Zaremba, Rowan Zellers, Chong Zhang, Marvin Zhang, Shengjia Zhao, Tianhao Zheng, Juntang Zhuang, William Zhuk, and Barret Zoph. 2024. Gpt-4 technical report. *Preprint*, arXiv:2303.08774.

K O'Shea. 2015. An introduction to convolutional neural networks. *arXiv preprint arXiv:1511.08458*.

Qizhi Pei, Lijun Wu, Kaiyuan Gao, Xiaozhuan Liang, Yin Fang, Jinhua Zhu, Shufang Xie, Tao Qin, and Rui Yan. 2024. BioT5+: Towards generalized biological understanding with IUPAC integration and multi-task tuning. In *Findings of the Association for Computational Linguistics: ACL 2024*, pages 1216–1240.

Abhispa Sahu and Jordan C Poler. 2024. Removal and degradation of dyes from textile industry wastewater: Benchmarking recent advancements, toxicity assessment and cost analysis of treatment processes. *Journal of Environmental Chemical Engineering*, page 113754.

Marwin H. S. Segler, Mike Preuss, and Mark P. Waller. 2018. Planning chemical syntheses with deep neural networks and symbolic AI. 555(7698):604–610.

M.B. Smith and J. March. 2007. *March's Advanced Organic Chemistry: Reactions, Mechanisms, and Structure*. Wiley.

Yuxuan Song, Jingjing Gong, Minkai Xu, Ziyao Cao, Yanyan Lan, Stefano Ermon, Hao Zhou, and Wei-Ying Ma. 2024. Equivariant flow matching with hybrid probability transport for 3d molecule generation. *Advances in Neural Information Processing Systems*, 36.

Mohammadamin Tavakoli, Pierre Baldi, Ann Marie Carlton, Yin Ting Chiu, Alexander Shmakov, and David Van Vranken. 2024. Ai for interpretable chemistry: predicting radical mechanistic pathways via contrastive learning. *Advances in Neural Information Processing Systems*, 36.

Junsu Ko Umit V. Ucak, Taek Kang and Juyong Lee. 2021. Substructure-based neural machine translation for retrosynthetic prediction. *Journal of Cheminformatics*, 13.

Yann Vander Meersche, Gabriel Cretin, Aria Gheeraert, Jean-Christophe Gelly, and Tatiana Galochkina. 2024. Atlas: protein flexibility description from atomistic molecular dynamics simulations. *Nucleic acids research*, 52(D1):D384–D392.

A Vaswani. 2017. Attention is all you need. *Advances in Neural Information Processing Systems*.

W. Patrick Walters and Regina Barzilay. 2021. Applications of deep learning in molecule generation and molecular property prediction. *Accounts of Chemical Research*, 54(2):263–270.

Yabing Wang, Zhuotao Tian, Qingpei Guo, Zheng Qin, Sanping Zhou, Ming Yang, and Le Wang. 2024. Referencing where to focus: Improving visualgrounding with referential query. *Preprint*, arXiv:2412.19155.

Tung-Yu Wu, Sheng-Yu Huang, and Yu-Chiang Frank Wang. 2024. Dora: 3d visual grounding with order-aware referring. *arXiv preprint arXiv:2403.16539*.

Zhenqin Wu, Bharath Ramsundar, Evan N Feinberg, Joseph Gomes, Caleb Geniesse, Aneesh Pappu, Karl Leswing, and Vijay Pande. 2017. Moleculenet: A benchmark for molecular machine learning. *Chemical Science*, 9.

Zonghan Wu, Shirui Pan, Fengwen Chen, Guodong Long, Chengqi Zhang, and S Yu Philip. 2020. A comprehensive survey on graph neural networks. *IEEE transactions on neural networks and learning systems*, 32(1):4–24.

Linhui Xiao, Xiaoshan Yang, Xiangyuan Lan, Yaowei Wang, and Changsheng Xu. 2024. Towards visual grounding: A survey. *arXiv preprint arXiv:2412.20206*.

Youjun Xu, Kangjie Lin, Shiwei Wang, Lei Wang, Chenjing Cai, Chen Song, Luhua Lai, and Jianfeng Pei. 2019. Deep learning for molecular generation. 11(6):567–597.

Di Zhang, Wei Liu, Qian Tan, Jingdan Chen, Hang Yan, Yuliang Yan, Jiatong Li, Weiran Huang, Xiangyu Yue, Dongzhan Zhou, Shufei Zhang, Mao Su, Han sen Zhong, Yuqiang Li, and Wanli Ouyang. 2024a. Chemllm: A chemical large language model. *ArXiv*, abs/2402.06852.

Haohui Zhang, Juntong Wu, Shichao Liu, and Shen Han. 2024b. A pre-trained multi-representation fusion network for molecular property prediction. *Information Fusion*, 103:102092.

A Appendix

A.1 Molecular Captioning Prompt Template

$f_{general}(IUPAC, SMILES)$: Given a molecular IUPAC name and its SMILES, your task is to provide a detailed description, including Basic Structure, Functional Groups, Stereochemistry, Molecular Size and Shape, Physicochemical Properties, Reactivity, Safety and Environmental Impact, etc.

$f_{publication}(literature)$: Given a molecular literature, extract the following information from the literature: 1) Physicochemical Properties: includes physicochemical characteristics of the molecule such as hole mobility, molecular weight, solubility, boiling point, melting point, pKa value (acid dissociation constant), and logP (lipophilicity); 2)Safety Information: Provides information regarding the safety of the molecule, such as its toxicity, carcinogenic, teratogenic, or mutagenic properties. 3) Application Areas: Provides an overview of the applications of the molecule. 4) Spectroscopic Properties: include spectroscopic data of the molecule, such as UV-visible absorption spectrum, infrared spectrum, nuclear magnetic resonance spectrum, and mass spectrometry data

$f_{specific}(StructureImage, SMILES)$: Given a molecular structure image and SMILES, generate a detailed molecular description (within 100 words) focusing number of rings, their types, and associated properties.

$f_{summarize}(f_{general}, f_{paper}, f_{specific})$: Given a molecular structure image, SMILES, IUPAC and three initial descriptions, summarize them and generate a molecular description focusing on basic structure, how substructures connect, and outlining their properties. following the example provided below. $Examples$

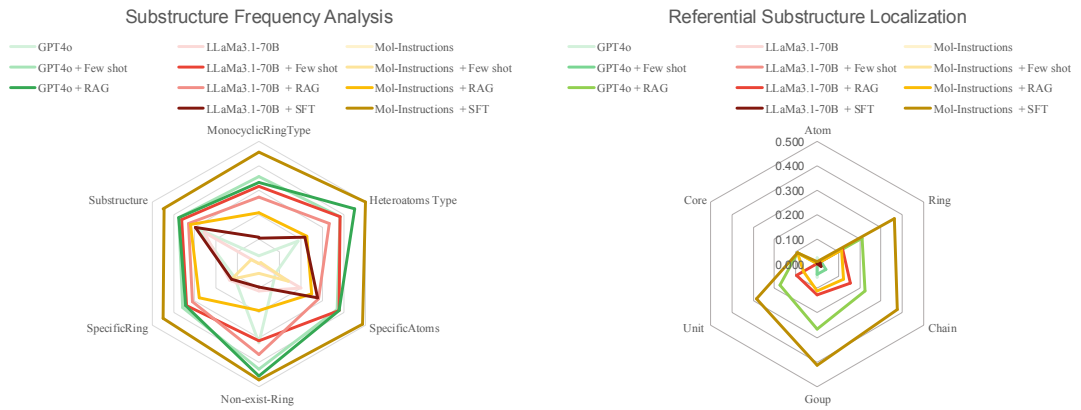

Figure 7: Performance on fine-grained types and structures.

A.2 Evaluation Metrics

For CNER, we report the F1-score of the multi-entity prediction and ground truth. For BNSM, SRG and SFA, we report accuracy. For RSL, we perform both substructure- and molecular-levels evaluation and report F1-score, IoU, accuracy and the substructure coverage. For the substructure-level evaluation, we evaluate the ground performance of each instance of each substructure one by one. As a substructure could have multiple instances in a molecule, we perform Hungarian matching to find the optical matches and evaluate on the best possible matches. Specifically, we compute the node IoU between grounding prediction and its ground truth of a substructure (i.e., local IoU IoU_l) and use it as the Hungarian cost function. We report precision, recall, and F1-score ($F1_l$) with $IoU_l = \{1, 0.7, 0.5\}$, where $IoU_l = 1$ represents an exact match between the ground truth and the prediction, and $IoU_l = 0.7$ (or 0.5) indicates 70% (or 50%) of node coverage. For the molecule-level evaluation, we treat all the predictions of a substructure as a whole and compare it with the ground truth annotation. Specifically, the molecule is seen as a graph where atom as node and their bonds as edge, and the grounding task is a node binary classification task. Specifically, the nodes belonging to the mentioning substructures should be highlighted (i.e., label=1). Otherwise, they should have the label of 0. Assuming that the ground truth label for a substructure in the molecule with m atoms is $y = [y_1, ..., y_m]$ and the predicted node classification as $\hat{y} = [\hat{y}_1, ..., \hat{y}_m]$, we compute the average accuracy of the node classification as the global evaluation metric as:

$$Acc_g = \frac{\#correctPrediction}{\#atoms} = \frac{|\hat{y}_i = y_i|}{m} \quad (6)$$

We also compute the IoU of the substructure $S = \{a_i | y_i = 1\}$ and the predicted highlight nodes $P = \{a_i | \hat{y}_i = 1\}$ as another global metric:

$$IoU_g = \frac{S \cap P}{S \cup P} \quad (7)$$

Besides, for the multiple substructure grounding task, we also report the substructure coverage rate Cov_s.

A.3 Fine-grained Performance

We also visualize the comparison on fine-grained level in Figure 7. The ICL and SFT significantly improve the SFA results on all types of counting tasks. The best-performing model is Mol-Instructions with SFT, which has over 0.9% on all dimensions. For the RSL, all models perform poorly at the atom and core grounding.